Communications in Mathematics and Applications
Vol. 17, No. 1, pp. 223–234, 2026
ISSN 0975-8607 (online); 0976-5905 (print)
Published by RGN Publications
DOI: 10.26713/cma.v17i1.3236

http://www.rgnpublications.com

Research Article

Investigating the Basin of Attraction and Sensitivity of SIQR-QS-QI Model

Sarita Jha[1], Prabhat Kumar Mandal[2], Govind Kumar Jha*[2] and Chandra Roy[2]

[1] *Department of Mathematics, K.B. Women's College, Hazaribagh 825301, Jharkhand, India*
[2] *University Department of Mathematics, Vinoba Bhave University, Hazaribagh 825301, Jharkhand, India*
***Corresponding author:** jhagovi@gmail.com

Received: June 22, 2025 **Revised:** August 15, 2025 **Accepted:** August 30, 2025

Abstract. This study presents the creation and analysis of a deterministic SIQR epidemic model that depicts how susceptible and infectious individuals interact with others who have been quarantined. The model demonstrates the key structure of disease transmission during quarantine processing. The stability properties of both the *disease-free equilibrium* (DFE) and *endemic equilibrium* (EE) were investigated using linearization via the Jacobian matrix and nonlinear analysis through Lyapunov's method. A sensitivity study of the reproductive number (R_0) was performed to determine the most influential parameters affecting disease dynamics and control. We additionally provide a guaranteed estimate of the basin of attraction for the EE, which characterizes the initial conditions that result in the persistence of the disease. Numerical simulations are used to validate theoretical conclusions and explain how critical parameters affect disease progression. This study provides valuable insights that can support the enhancement of public health strategies and refinement of quarantine protocols.

Keywords. Equilibrium point, Stability, Reproduction number, Lyapunov function, Sensitivity analysis, Domain of attraction

Mathematics Subject Classification (2020). 92D30, 34D20,93A30, 37N25

1. Introduction

Infectious diseases have long threatened human health and social stability. From the Spanish flu in 1918 to the more recent COVID-19 pandemic, infectious disease outbreaks have illustrated how quickly a pathogen can spread and overwhelm global healthcare systems. The complexities of modern disease transmission, via air travel, urbanization, and social behavior, require more precise techniques for understanding and predicting disease dynamics. Multiple compartmental

models have been created to explain the behavior of endemics. Some popular models are SIS, SIR, SIRS, SEI, SEIR, and SIQR (see, Busenberg and van den Driessche [4], Butler *et al*. [5], Fenner *et al*. [9], Hethcote [11], Li and Wang [13], Li *et al*. [14]).

This SIQR-QS-QI model is a development of the original SIR model designed by Kermack and McKendrick [12] in 1927, incorporating quarantine as a key control mechanism. During the past two decades, numerous researchers have adapted and refined the SIQR model to study the effect of isolation and quarantine. Hethcote [11] presented a fundamental overview of mathematical models for infectious diseases, highlighting the significance of quarantine extensions. Gumel *et al*. [10] suggested an SIQR model that integrates isolation and quarantine into the SEIR framework in order to investigate the SARS outbreak in Toronto. During the H_1N_1 pandemic, Arino *et al*. [2] worked on SIQR and SEIQR models and studied vaccination and quarantine strategies. Yan and Zou [20] analyzed optimal quarantine and isolation strategies in disease control. Feng [8] introduced a time-dependent quarantine rate in a modified SEIR model for better control of infectious diseases. During the COVID-19 pandemic, Zhao and Chen [22] investigated the early dynamics of the COVID-19 epidemic using an SEIQR model. López and Rodó [15] introduced a time-dependent SIQR model for COVID-19 in Spain, incorporating additional compartments such as asymptomatic, hospitalized, and undetected individuals. Several studies have further explored the dynamics of COVID-19 and related infectious diseases through mathematical modelling approaches (see, Batistela *et al*. [3], and Wang *et al*. [18])

While previous models capture many aspects of disease control, most of them assume perfect quarantine, where quarantined individuals do not interact with the rest of the population. In a real-world scenario, such isolation is not possible. Quarantined individuals can come into contact with susceptible or infectious individuals through various means, such as family interactions, healthcare visits, or accidental exposure. Therefore, in this paper, we designed a compartmental model SIQR-QS-QI where the quarantine population can mix with susceptible and infectious individuals. Here, the population is assumed to have a uniform spatial distribution, people mix according to the law of mass action. Moreover, the transmission rates between susceptible, infected, and quarantine individuals are assumed to be constant, and we neglect the effects of external interventions like vaccination or changes in public health policies during the disease progression.

In Section 2, we describe our model and compute the basic reproduction number R_0. In Section 3, we extracted the disease-free equilibrium point and demonstrated its stability both locally and globally. In Section 4, we established the local and global stability of the endemic equilibrium point under specific circumstances. In Section 5, we have done the numerical simulation of our model, which proves the stability result of our proposed model. A sensitivity analysis can help find which parameters have the most influence on the spread of diseases, hence improving the efficiency of disease control strategies. So, sensitivity analysis has been done in Section 6, and the graph of it regarding each parameter of the model is there. We have estimated the domain of attraction of our model with the help of LPP in Section 7, and lastly, the paper concludes with a discussion in Section 8.

2. Description of Our Model

To gain a better comprehension and manage the regulation of infectious diseases, a mathematical framework of transmission dynamics must be developed. In this paper, we present a transmission model, SIQR-QS-QI, that includes quarantine and recovery phases to replicate

real-world disease management techniques. Figure 1 illustrates the transmission dynamics among compartments:

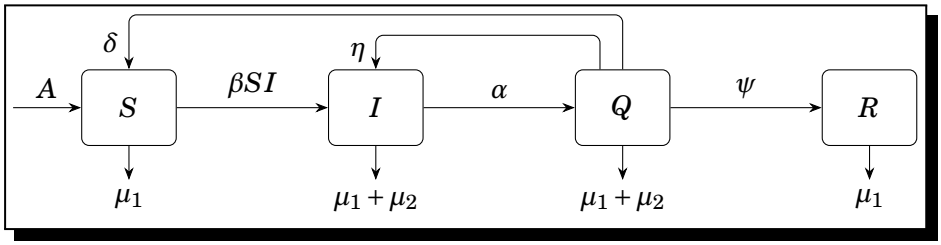

Figure 1. Disease transmission of our model

This model recruits incoming individuals into the susceptible class at a steady rate A. Susceptible persons acquire infection by effective contact with infected individuals, represented by the term βSI, where β is the mean action coefficient of transmission. Infected individuals leave their compartment, governed by the parameter α, to enter the quarantine class, where they may either progress to more severe infection governed by η, recover governed by the parameter ψ, or return to the susceptible class at rate δ. Natural death occurs at rate μ_1 across all compartments, and additional disease-related mortality occurs in the infected and quarantined classes at rate μ_2.

The parameters in this model have the following meanings:

A	:	Rate at which the susceptible population is recruited
β	:	Coefficient of transmission because susceptible and diseased people come into contact
μ_1	:	Per capita normal rate of death
μ_2	:	Disease-related death rate
α	:	Rate at which individuals with diseases are transferred to the quarantine area
η	:	The rate of serious infection among those under quarantine
ψ	:	Rate of recovery for those under quarantine
δ	:	Rate at which quarantined asymptomatic individuals are susceptible

Using the definitions, disease transmission flow and parameter assumptions following differential equations are formulated to describe the disease dynamics:

$$\left.\begin{aligned} \tfrac{dS}{dt} &= A - \beta SI - \mu_1 S + \delta Q, \\ \tfrac{dI}{dt} &= \beta SI - (\mu_1 + \mu_2 + \alpha) I + \eta Q, \\ \tfrac{dQ}{dt} &= \alpha I - (\mu_1 + \mu_2 + \eta + \delta + \psi) Q, \\ \tfrac{dR}{dt} &= \psi Q - \mu_1 R. \end{aligned}\right\} \tag{2.1}$$

Here, $S \geq 0$, $I \geq 0$, $Q \geq 0$, and $R \geq 0$ are assumed to hold in the feasible region. When the system is disease-free ($I = 0$, $Q = 0$), as $t \to \infty$, then $N \to \frac{A}{\mu_1}$. Thus, the DFE is $P_0\left(\frac{A}{\mu_1}, 0, 0, 0\right)$, and the solution of the given system (2.1) lies within the region

$$\Omega = \left\{ (S, I, Q, R) \in R_+^4 \;\middle|\; S + I + Q + R \leq \frac{A}{\mu_1} \right\}. \tag{2.2}$$

It is a well-posed initial value problem, as all solutions stay restricted to the positive invariant area Ω for all $t \geq 0$. Now, the next-generation matrix approach is employed to derive the basic

reproductive number for system (2.1) (see, Anderson and May [1], van den Driessche and Watmough [17]). It is the typical number of secondary infections that occur when an infectious agent enters a population that is completely susceptible (see, Mishra *et al*. [16]). It is indicated by R_0 and determined as the dominant eigenvalue of FV^{-1}. We get

$$R_0 = \rho(FV^{-1}) = \frac{\beta A(\mu_1+\mu_2+\eta+\delta+\psi)}{\mu_1[(\mu_1+\mu_2+\alpha)(\mu_1+\mu_2+\eta+\delta+\psi)-\alpha\eta]}. \tag{2.3}$$

3. DFE $\left(\frac{A}{\mu_1},0,0,0\right)$

We will discuss the stability when $R_0 < 1$. After finding its Jacobian matrix at DFE, we will prove all its eigenvalues posses negative real part. So, the jacobian matrix at $\left(\frac{A}{\mu_1},0,0,0\right)$ is

$$J(P_0) = \begin{bmatrix} -\mu_1 & -\frac{\beta A}{\mu_1} & \delta & 0 \\ 0 & \frac{\beta A}{\mu_1}-(\mu_1+\mu_2+\alpha) & \eta & 0 \\ 0 & \alpha & -(\mu_1+\mu_2+\eta+\delta+\psi) & 0 \\ 0 & 0 & \psi & -\mu_1 \end{bmatrix}.$$

Two eigenvalues $J(P_0)$ are $\lambda_1 = \lambda_2 = -\mu_1$, and the remaining two are given by the roots of

$$\lambda^2 + \left[(\mu_1+\mu_2+\eta+\delta+\psi) - \left(\frac{\beta A}{\mu_1}-(\mu_1+\mu_2+\alpha)\right)\right]\lambda$$
$$-\left[(\mu_1+\mu_2+\eta+\delta+\psi)\left(\frac{\beta A}{\mu_1}-(\mu_1+\mu_2+\alpha)\right)+\alpha\eta\right] = 0. \tag{3.1}$$

Using the Hurwitz criterion (Zhan and Hu [21]), for the quadratic equation (3.1), all roots have negative real parts iff $\Delta_1 > 0$ and $\Delta_2 > 0$, where

$$\Delta_1 = (\mu_1+\mu_2+\eta+\delta+\psi) - \left(\frac{\beta A}{\mu_1}-(\mu_1+\mu_2+\alpha)\right),$$
$$\Delta_2 = -\left[(\mu_1+\mu_2+\eta+\delta+\psi)\left(\frac{\beta A}{\mu_1}-(\mu_1+\mu_2+\alpha)\right)+\alpha\eta\right].$$

Hence, this DFE is locally asymptotically stable. Now, for global stability of DFE, we define a Lyapunov function,

$$L_1 = (\psi+\eta+\delta+\mu_1+\mu_2)I + \eta Q \geq 0,$$

therefore,

$$\begin{aligned}\dot{L}_1 &= [\beta S(\mu_1+\mu_2+\eta+\delta+\psi) - (\mu_1+\mu_2+\alpha)(\mu_1+\mu_2+\eta+\delta+\psi)]I \\ &\quad + \eta Q(\mu_1+\mu_2+\eta+\delta+\psi) + \alpha\eta I - \eta(\mu_1+\mu_2+\eta+\delta+\psi)Q \\ &= [\beta S(\mu_1+\mu_2+\eta+\delta+\psi) + \alpha\eta - (\mu_1+\mu_2+\alpha)(\mu_1+\mu_2+\eta+\delta+\psi)]I \\ &\leq 0 \qquad \text{(because } I \geq 0 \text{ and } R_0 \leq 1\text{)}.\end{aligned}$$

Since, $S \leq \frac{A}{\mu_1}$ so by Lyapunov-Lasalle's theorem (Li *et al*. [13, 14]), solution in Ω approaches the maximal positively invariant portion of the region where $I = 0$ and also when $t \to \infty$, then $Q \to 0$, thus, $\frac{dS}{dt} = A - \mu_1 s$ implies $S \to \frac{A}{\mu_1}$. Thus, all solution in the set where $I = 0$ tends to DFE $\left(\frac{A}{\mu_1},0,0,0\right)$. We can state this in a theorem as follows.

Theorem 3.1. *If $R_0 < 1$ in the system* (2.1) *then* Ω (2.2) *is an asymptotically stable region for* $(\frac{A}{\mu_1},0,0,0)$. *Also, by Lyapunov-LaSalle's theorem, DFE is globally asymptotically stable since L_1 is radially unbounded.*

4. Endemic Equilibrium (EE)

Here, $I \neq 0$ therefore, $Q \neq 0$, $R \neq 0$. For EE, put $\frac{dS}{dt} = \frac{dI}{dt} = \frac{dQ}{dt} = \frac{dR}{dt} = 0$ in the system (2.1) and on solving those equations, we get,

$$\left.\begin{aligned} S^* &= k_3 = \tfrac{\mu_1+\mu_2+\alpha-\eta k_1}{\beta}, \\ Q^* &= k_1 k_4, \\ I^* &= k_4 = \tfrac{\mu_1 k_3 - A}{\delta k_1 - \beta k_3}, \\ R^* &= k_2 k_4, \end{aligned}\right\} \tag{4.1}$$

where $k_1 = \frac{\alpha}{\mu_1+\mu_2+\eta+\delta+\psi}$, $k_2 = \frac{\psi}{\mu_1} k_1$, $k_3 = \frac{(\mu_1+\mu_2+\alpha)-\eta k_1}{\beta}$, $k_4 = \frac{\mu_1 k_3 - A}{\delta k_1 - \beta k_3}$.
Hence, (S^*, I^*, Q^*, R^*) is the endemic equilibrium point. After finding its Jacobian matrix, it is quite similar, as discussed in Section 3, to prove its local stability by the Hurwitz theorem (Zhan and Hu [21]); hence, this part is omitted. Now, the global dynamic behavior of the EE is established using a Lyapunov function. To construct the Lyapunov function at EE, we will shift the origin to make our equilibrium point $(0,0,0,0)$. Put $S = S' + S^*$, $Q = Q' + Q^*$, $I = I' + I^*$ and $R = R' + R^*$ in system (2.1), we get

$$\left.\begin{aligned} \tfrac{dS'}{dt} &= -\beta S'I' - \beta S'I^* - \beta S^*I' - \mu_1 S' + \delta Q', \\ \tfrac{dI'}{dt} &= \beta S'I' + \beta S'I^* + \beta S^*I' - (\mu_1+\mu_2+\alpha)I' + \eta Q', \\ \tfrac{dQ'}{dt} &= \alpha I' - (\mu_1+\mu_2+\eta+\delta+\psi)Q', \\ \tfrac{dR'}{dt} &= \psi Q' - \mu_1 R'. \end{aligned}\right\} \tag{4.2}$$

Let the Lyapunov function be, $L_2 = S' + I' + Q' + R'$, such that

$$\begin{aligned} \dot{L}_2 &= \dot{S}' + \dot{I}' + \dot{Q}' + \dot{R}' \\ &= -\beta S'I' - \beta S'I^* - \beta S^*I' - \mu_1 S' + \delta Q' \beta S'I' + \beta S'I^* + \beta S^*I' \\ &\quad -(\mu_1+\mu_2)I' + \alpha I' - (\mu_1+\mu_2)Q' - \eta Q' - \delta Q' - \psi Q' + \psi Q' - \mu_1 R' \\ &= -\mu_1 S' - \mu_1 I' - \mu_1 Q' - \mu_1 R' - \mu_2 I' - \mu_2 Q' < 0 \\ &= -\mu_1(S' + I' + Q' + R') - \mu_2(I' + Q') < 0. \end{aligned}$$

Since L_2 is radially unbounded, and $\dot{L}_2$ is negative. Thus, by Lasalle's theorem, it is globally asymptotically stable. Hence, we can state this in a theorem as:

Theorem 4.1. *The EE point* (S^*, I^*, Q^*, R^*) *of system* (2.1) *satisfying the coordinates* (4.1) *is asymptotically stable in the region* Ω (2.2) *when* $R_0 > 1$.

5. Numerical Simulation

Numerical simulations are used to predict the long-term behavior of the epidemic under various intervention scenarios, so numerical simulations of the endemic equilibrium of our model are carried out in this section. The system (2.1) is solved numerically using the adaptive Runge-Kutta method (ODE45) implemented in MATLAB (R2024a). This method ensures stability and accuracy in capturing the dynamics of the epidemic over time. The parameter value used for this simulation is presented in Table 1. Parameter values are assumed on the basis of realistic epidemiological settings that satisfy $R_0 > 1$. Since our system is four-dimensional, we plot their projections in a three-dimensional system. In Figure 2, we observed that all trajectories

of system (2.1) starting from different initial values converge to a unique EE point in each projection (see Figure 2(a,b,c,d)). So, the EE point $P^*(S^*,I^*,Q^*,R^*)$ satisfying the coordinates (4.1) is asymptotically stable when $R_0 > 1$ in region Ω.

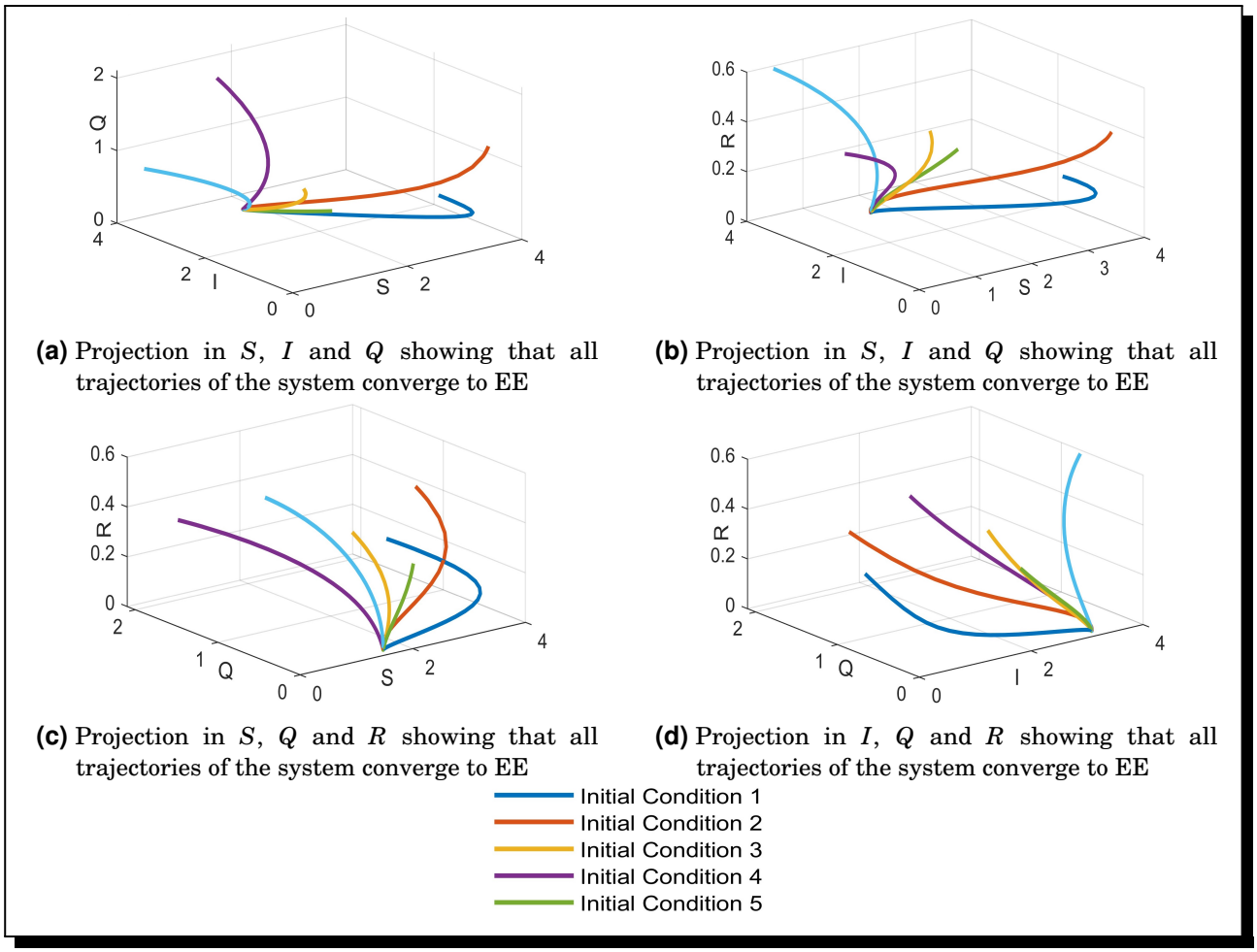

(a) Projection in S, I and Q showing that all trajectories of the system converge to EE

(b) Projection in S, I and Q showing that all trajectories of the system converge to EE

(c) Projection in S, Q and R showing that all trajectories of the system converge to EE

(d) Projection in I, Q and R showing that all trajectories of the system converge to EE

Figure 2. A MATLAB plot of different 3D projections of our 4D system (2.1), parametric values are taken from Table 1, showing the dynamical relation among S,I,Q and R under varying initial condition

Table 1. Parameter's value for EE

Parameters	Value
β	0.2
A	1.5
μ_1	0.3
μ_2	0.01
η	0.03
δ	0.02
ψ	0.02
α	0.01

6. Sensitivity Analysis

To assess the relative significance of different parameters in their effect on disease patterns, we carried out a sensitivity analysis of (R_0). The quantity R_0 is an essential threshold parameter that determines whether the disease will replicate or stay inside the community. So, investigating its sensitivity with regard to the model's parameters aids in determining the parameters for effective disease control. This was accomplished by using the forward normalized sensitivity index. This sensitivity index of R_0 with regard to a parameter (p) is quantified by Chitnis *et al*. [7],

$$S_p^{R_0} = \frac{\partial R_0}{\partial p}\frac{p}{R_0}.$$

These sensitivity indices indicate whether parameters in our model have a strong or weak influence on the R_0 or disease transmission. Using the baseline parameter values from Table 1, we have calculated the sensitivity indices for all the parameters involved in the expression of R_0, including the $\beta, A, \mu_1, \mu_2, \eta, \delta, \psi$, and α. Table 2 lists the sensitivity indices of R_0 for each model parameters η, μ_1, μ_2, and α are negative.

Table 2. Sensitivity indices

Parameters	Baseline	Sensitivity
β	0.2	1
A	1.5	1
μ_1	0.3	−1.9418
μ_2	0.01	−0.0314
α	0.01	−0.0289
η	0.03	−0.0023
δ	0.02	0.00013
ψ	0.02	0.00013

As a result, R_0 decreases when the value of these parameters increases. On the other hand, R_0's sensitivity indices to the parameters β, A, δ, and ψ are positive, indicating that any increment in these parameters causes R_0 to grow. To visualize how R_0 changes with respect to each parameter, we draw MATLAB-based plots by varying one parameter at a time while keeping others constant at baseline values (see Figure 3).

7. Basin of Attraction (BOA)

The set of all beginning conditions $x_0 \in R^n$ for which the trajectories $x(t)$ of a dynamical system satisfy $x(t)$ tending to x^* as t tends to ∞ is known as the BOA $\mathcal{D}(x^*)$ of an equilibrium point x^* in that system (see, Chen *et al*. [6]). For example, the system $x' = f(x)$ has a BOA of x^* that can be represented as

$$\mathcal{D}(x^*) = \left\{x_0 \in R^n \ : \ \lim_{t\to\infty} x(t;x_0) = x^*\right\}. \tag{7.1}$$

The BOA for $x' = f(x)$; $x(0) = x_0$ may be guaranteed to be estimated as [19]

$$\mathcal{D}(x^*) = \{x : V(x) < C\}, \tag{7.2}$$

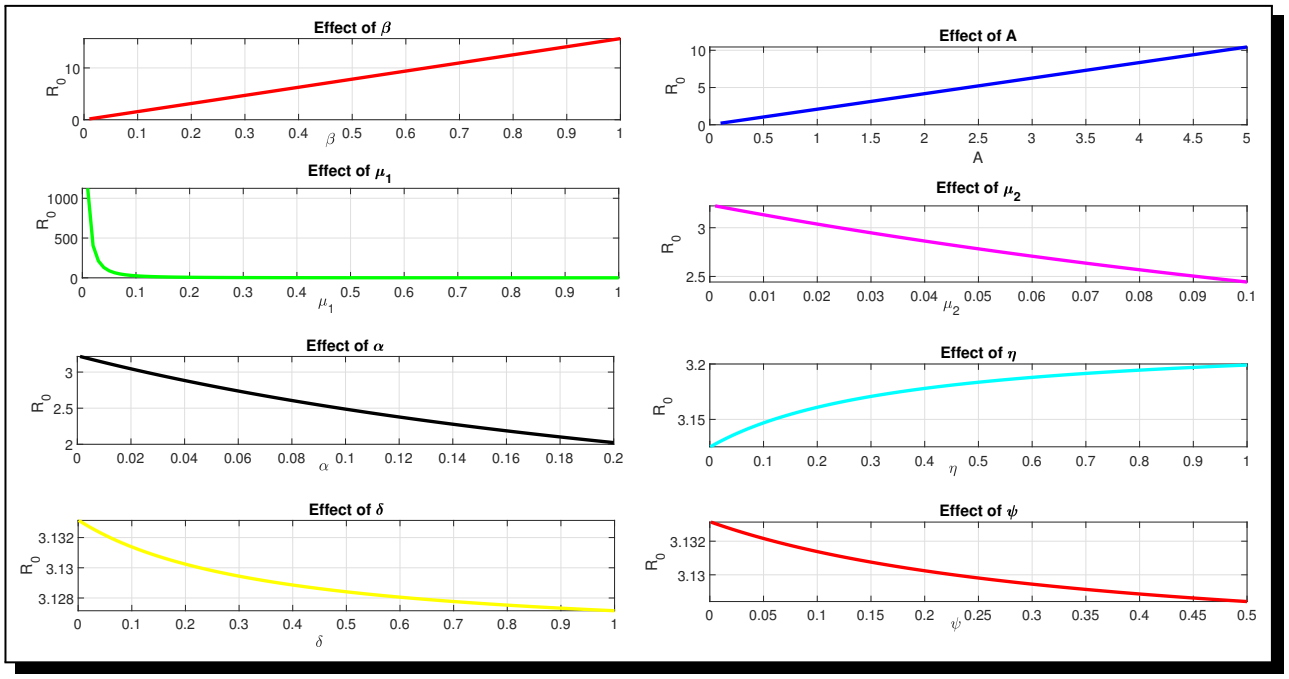

Figure 3. MATLAB-based variation plots of R_0 with respect to key model parameters. Each subplot demonstrates the sensitivity of R_0 toward a specific parameter

where $V(x)$ is the Lyapunov function. We have to find the maximum value of C; for this, we will solve the LPP,

$$C = \min V(x), \quad \dot{V} < 0,\ x \neq 0. \tag{7.3}$$

Suppose $R = 0$, then $\frac{dR}{dt} = 0$ implies $\psi = 0$, and our original system reduces in the three dimensional system. The EE of this reduced system $(S^*,\ I^*,\ Q^*)$ shifted to the origin for making our EE point $(0,0,0)$ by substituting $S = S' + S^*$, $I = I' + I^*$ and $Q = Q' + Q^*$, we get the system (4.2). Substituting the parameters value in (4.2), we get the transformed system as

$$\left.\begin{aligned} \frac{dS'}{dt} &= 0.2\ S'I' - 0.2\ S'I^* - 0.2\ S^*I' - 0.3\ S' + 0.02\ Q', \\ \frac{dI'}{dt} &= 0.2\ S'I' + 0.2\ S'I^* + 0.2\ S^*I' - 0.32\ I' + 0.03\ Q', \\ \frac{dQ'}{dt} &= 0.01\ I' - 0.36\ Q'. \end{aligned}\right\} \tag{7.4}$$

Lyapunov function of the system (7.4) is,

$$V = S' + I' + Q',$$

$$\dot{V} = -0.3\ S' - 0.31I' - 0.31\ Q',$$

and, from feasible region (2.2), we got $S' + I' + Q' < 0.112$. So, the following LPP will give the value of C^*,

$$C^* = \min\{S' + I' + Q'\},$$

subject to constraints

$$-0.3\ S' - 0.31I' - 0.31\ Q' < 0,$$

$$S' + I' + Q' < 0.112,$$

$$S',\ I',\ Q' \geq 0.$$

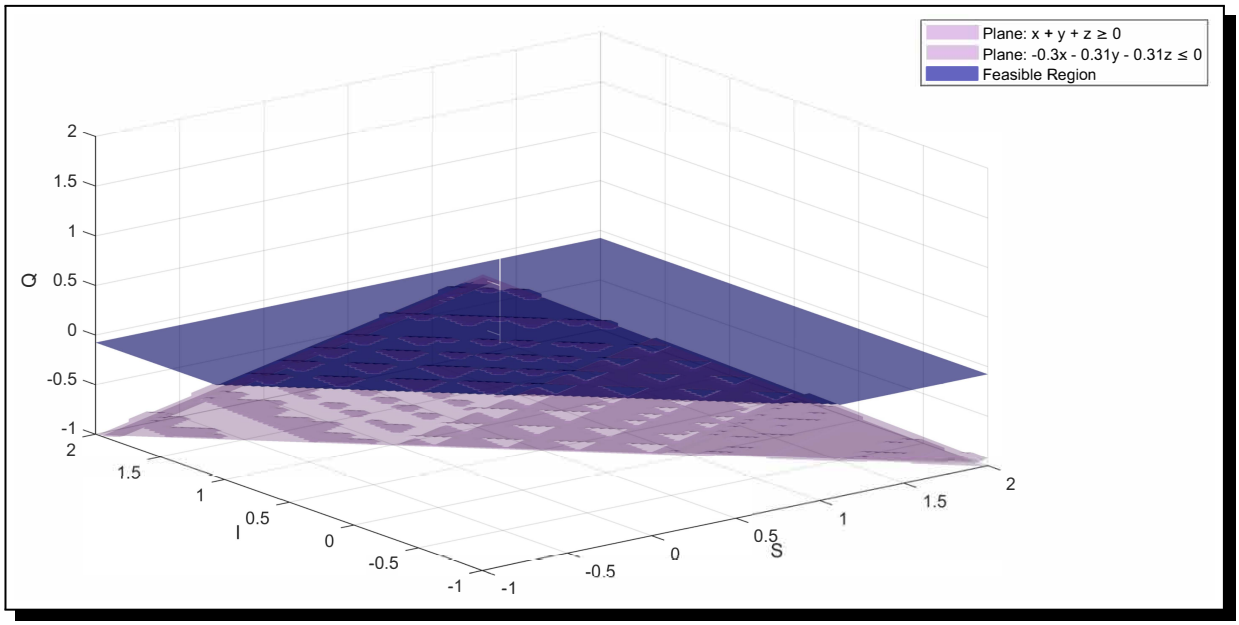

Figure 4. MATLAB-based 3D visualization of the basin of attraction for EE of our model. The shaded region, shown in dark blue, represents the BOA

On solving this LPP, we get $C^* = 0$. Hence, the BOA is given by the bounded region of

$$\left.\begin{aligned} &S' + I' + Q' > 0, \\ &-0.3\,S' - 0.31\,I' - 0.31\,Q' < 0, \\ &S' > -1.596,\ \ I' > -3.205,\ \ Q' > -0.087. \end{aligned}\right\} \tag{7.5}$$

See Figure 4, the feasible region enclosed between two planes in the (S,I,Q) phase space demonstrates the region of initial conditions for which the system trajectories converge to a unique EE, and the shaded region in dark blue is the required BOA.

8. Conclusions

In this study, we proposed an endemic model SIQR-QS-QI with constant recruitment into the susceptible class and analyzed its local and global dynamics. It was demonstrated that the DFE and EE are locally asymptotically stable when $R_0 < 1$ and $R_0 > 1$ respectively. The global stability of both equilibria was established via LaSalle's invariance principle and Lyapunov functions, respectively.

We have performed a numerical simulation to prove the stability results of our model. Through sensitivity analysis, we found that R_0 is strongly sensitive to the contact rate of infectious people β, the recruitment rate A, and natural mortality μ_1. The parameters μ_1, μ_2, α, and η have negative sensitivity indices of R_0, which means that increasing their values will result in a decrease in R_0 or the spread of disease, and the sensitivity indices of R_0 to the parameters β, A, δ and ψ are positive, which means that an increase in the value of these parameters leads to an increase in R_0 or the transmission of disease.

A major contribution of this work lies in the basin of attraction analysis, derived both analytically and graphically. A *Linear Programming Problem* (LPP) was formulated to identify a feasible region in the (S,I,Q)-phase space where all trajectories of the system converge to the EE. This improves our understanding of the initial conditions required for stability. The model

effectively captures quarantine dynamics and multiple infectious stages, making it suitable for studying diseases influenced by isolation policies.

Our model structure captures key features of epidemic progression, including quarantine dynamics, making it suitable for analyzing diseases where isolation and intervention policies play a significant role. However, it relies on simplifying assumptions such as homogeneous mixing, constant parameters, and literature-based values, and does not account for behavioral changes, spatial heterogeneity, seasonal effects, or real-time data calibration, which may limit predictive accuracy. Despite these limitations, the model provides practical insights by enabling evaluation of quarantine and isolation strategies, supporting resource allocation such as hospital beds, testing capacity, and vaccination planning, and simulating different intervention scenarios. Furthermore, the framework can be adapted to study other infectious diseases where quarantine and isolation play a crucial role. Future work may focus on extending the model by incorporating vaccination, age structure, stochastic effects, and real epidemiological data to enhance predictive precision and practical applicability.

Nomenclature

Abbreviation/Symbol	Description
DFE	Disease-Free Equilibrium
EE	Endemic Equilibrium
BOA	Basin of Attraction
LPP	Linear Programming Problem
LAS	Local Asymptotic Stability
GAS	Global Asymptotic Stability
SIQR-QS-QI	Susceptible-Infectious-Quarantined-Recovered-Quarantined Susceptible-Quarantined Infectious
SARS	Severe Acute Respiratory Syndrome
COVID-19	Coronavirus Disease 2019
WHO	World Health Organization
S	Susceptible population
I	Infectious population
Q	Quarantined population
R	Recovered population
R_0	Basic reproduction number
J	Jacobian matrix
L_1	Lyapunov function for DFE point
L_2	Lyapunov function for EE point
Ω	Feasible region of the system

Note. Detailed definitions of the model parameters $(A, \beta, \alpha, \eta, \delta, \psi, \mu_1, \mu_2)$ are provided in Section 2.

Competing Interests

The authors declare that they have no competing interests.

Authors' Contributions

All the authors contributed significantly in writing this article. The authors read and approved the final manuscript.

References

[1] R. M. Anderson and R. M. May, Population biology of infectious diseases: Part I, *Nature* **280** (1979), 361 – 367, DOI: 10.1038/280361a0.

[2] J. Arino, F. Brauer, P. van den Driessche, J. Watmough and J. Wu, A final size relation for epidemic models, *Mathematical Biosciences and Engineering* **4**(2) (2007), 159 – 175, DOI: 10.3934/mbe.2007.4.159.

[3] C. M. Batistela, D. P.F. Correa, Á. M. Bueno and J. R. C. Piqueira, SIRSi compartmental model for COVID-19 pandemic with immunity loss, *Chaos, Solitons & Fractals* **142** (2021), 110388, DOI: 10.1016/j.chaos.2020.110388.

[4] S. Busenberg and P. van den Driessche, Analysis of a disease transmission model in a population with varying size, *Journal of Mathematical Biology* **28** (1990), 257 – 270, DOI: 10.1007/BF00178776.

[5] G. Butler, H. Freedman and P. Waltman, Uniformly persistent systems, *Proceedings of the American Mathematical Society* **96** (1986), 425 – 430.

[6] X. Chen, J. Cao, J. H. Park and J. Qiu, Stability analysis and estimation of domain of attraction for the endemic equilibrium of an SEIQ epidemic model, *Nonlinear Dynamics* **87** (2017), 975 – 985, DOI: 10.1007/s11071-016-3092-7.

[7] N. Chitnis, J. M. Hyman and J. M. Cushing, Determining important parameters in the spread of malaria through the sensitivity analysis of a mathematical model, *Bulletin of Mathematical Biology* **70** (2008), 1272 – 1296, DOI: 10.1007/s11538-008-9299-0.

[8] Z. Feng, Final and peak epidemic sizes for SEIR models with quarantine and isolation, *Mathematical Biosciences and Engineering* **4** (2007), 675 – 686, DOI: 10.3934/mbe.2007.4.675.

[9] F. Fenner, D. A. Henderson, I. Arita, Z. Jezek and I. D. Ladnyi, Smallpox and its eradication, Smallpox and its eradication, in: *History of International Public Health*, Number 6, World Health Organization, 1460 pages (1998), URL: https://iris.who.int/handle/10665/39485.

[10] A. B. Gumel, S. Ruan, T. Day, J. Watmough, F. Brauer, P. van den Driessche, D. Gabrielson, C. Bowman, M. E. Alexander, S. Ardal, J. Wu and B. M. Sahai, Modelling strategies for controlling SARS outbreaks, *Proceedings of the Royal Society of London. Series B* **271**(1554) (2004), 2223 – 2232, DOI: 10.1098/rspb.2004.2800.

[11] H. W. Hethcote, The mathematics of infectious diseases, *SIAM Review* **42**(4) (2000), 599 – 653, DOI: 10.1137/S0036144500371907.

[12] W. O. Kermack and A. G. McKendrick, A contribution to the mathematical theory of epidemics, *Proceedings of the Royal Society of London. Series A* **115**(772) (1927), 700 – 721, DOI: 10.1098/rspa.1927.0118.

[13] M. Y. Li and L. Wang, Global stability in some SEIR epidemic models, in: *Mathematical Approaches for Emerging and Reemerging Infectious Diseases: Models, Methods, and Theory*, C. Castillo-Chavez, S. Blower, P. van den Driessche, D. Kirschner and A. A. Yakubu (editors), *The IMA Volumes in Mathematics and its Applications*, Vol. 126, Springer, New York, pp. 295 – 311, (2002), DOI: 10.1007/978-1-4613-0065-6_17.

[14] M. Y. Li, J. R. Graef, L. Wang and J. Karsai, Global dynamics of a SEIR model with varying total population size, *Mathematical Biosciences* **160**(2) (1999), 191 – 213, DOI: 10.1016/S0025-5564(99)00030-9.

[15] L. López and X. Rodó, The end of social confinement and COVID-19 re-emergence risk, *Nature Human Behaviour* **4** (2020), 746 – 755, DOI: 10.1038/s41562-020-0908-8.

[16] B. K. Mishra, A. K. Keshri, D. K. Saini, S. Ayesha, B. K. Mishra and Y. S. Rao, Mathematical model, forecast and analysis on the spread of COVID-19, *Chaos, Solitons & Fractals* **147** (2021), 110995, DOI: 10.1016/j.chaos.2021.110995.

[17] P. van den Driessche and J. Watmough, Reproduction numbers and sub-threshold endemic equilibria for compartmental models of disease transmission, *Mathematical Biosciences* **180**(1-2) (2002), 29 – 48, DOI: 10.1016/S0025-5564(02)00108-6.

[18] S. Wang, Y. Pan, Q. Wang, H. Miao, A. N. Brown and L. Rong, Modeling the viral dynamics of SARS-CoV-2 infection, *Mathematical Biosciences* **328** (2020), 108438, DOI: 10.1016/j.mbs.2020.108438.

[19] S. Warthenpfuhl, B. Tibken and S. Mayer, An interval arithmetic approach for the estimation of the domain of attraction, in: *2010 IEEE International Symposium on Computer-Aided Control System Design* (Yokohama, Japan, 2010), pp. 1999 – 2004, (2010), DOI: 10.1109/CACSD.2010.5612692.

[20] P. Yan and Y. Zou, Optimal and sub-optimal quarantine and isolation control in SARS epidemics, *Mathematical and Computer Modelling* **47**(1-2) (2008), 235 – 245, DOI: 10.1016/j.mcm.2007.04.003.

[21] X. Zhan and Y. Hu, On the relation between Hurwitz stability of matrix polynomials and matrix-valued Stieltjes functions, *Journal of Computational and Applied Mathematics* **417** (2023), 114614, DOI: 10.1016/j.cam.2022.114614.

[22] S. Zhao and H. Chen, Modeling the epidemic dynamics and control of COVID-19 outbreak in China, *Quantitative Biology* **8**(1) (2020), 11 – 19, DOI: 10.1007/s40484-020-0199-0.